Thermochromic effect at room temperature of Sm0.5Ca0.5MnO3 thin films

Alexis Boileau, Fabien Capon, Silvère Barrat, Patrick Laffez, J. F. Pierson

Thermochromic effect at room temperature of $Sm_{0.5}Ca_{0.5}MnO_3$ thin films

Cite as: J. Appl. Phys. **111**, 113517 (2012); https://doi.org/10.1063/1.4722264
Submitted: 24 April 2012 . Accepted: 25 April 2012 . Published Online: 06 June 2012

A. Boileau, F. Capon, S. Barrat, P. Laffez, and J. F. Pierson

Thermochromic effect at room temperature of $Sm_{0.5}Ca_{0.5}MnO_3$ thin films

A. Boileau,[1] F. Capon,[1,a)] S. Barrat,[1] P. Laffez,[2] and J. F. Pierson[1]
[1]*Université de Lorraine, Institut Jean Lamour, Département CP2S, UMR CNRS 7198, Nancy, F-54042, France*
[2]*Groupe de Recherche Electronique, Matériaux, Acoustique, Nanoscience (GREMAN), Université François Rabelais de Tours, UMR CNRS 7347, IUT de Blois, 15 rue de la Chocolaterie, Blois, F-41000, France*

(Received 24 April 2012; accepted 25 April 2012; published online 6 June 2012)

$Sm_{0.5}Ca_{0.5}MnO_3$ thermochromic thin films were synthesized using dc reactive magnetron co-sputtering and subsequent annealing in air. The film structure was studied by x-ray diffraction analysis. To validate the thermochromic potentiality of $Sm_{0.5}Ca_{0.5}MnO_3$, electrical resistivity and infrared transmittance spectra were recorded for temperatures ranging from 77 K to 420 K. The temperature dependence of the optical band gap was estimated in the near infrared range. Upon heating, the optical transmission decreases in the infrared domain showing a thermochromic effect over *a wide wavelength* range at room temperature. © *2012 American Institute of Physics*. [http://dx.doi.org/10.1063/1.4722264]

I. INTRODUCTION

Manganese perovskites $A_xB_{1-x}MnO_3$ where A (A = La, Pr, Nd, Sm…) is a trivalent cation of the lanthanide series and B (B = Ba, Sr, Ca…) a divalent cation are subjected to significant developments due to their large range of combined thermal, electrical, and magnetic properties. Among these oxides, $Sm_xCa_{1-x}MnO_3$ (SCMO) would open numerous applications based on negative colossal magnetoresistance, thermoelectric power, and decontaminating electrodes for leachates treatments.[1–3] The properties of SCMO have been intensively studied but few of them concern its optical and infrared (IR) behavior. Recently, Laffez *et al.*[4,5] and Ammar *et al.*[6] presented $Sm_{0.35}Ca_{0.65}MnO_3$ as a temperature modulated infrared optical switches. This last item so-called thermochromic effect based on a charge order (CO) transition versus temperature is a real challenge in the domain of the passive thermal regulation and the infrared discretion.[5]

This work is motivated by diversification and optimization of potential thermochromic materials in different transparency bands of the atmosphere corresponding to the wavelength ranges 1–2.8 μm (band I), 3–5 μm (band II), and 8–14 μm (band III). Some applications like infrared detection materials and devices need materials which are optically active in these domains while keeping a good contrast between the transparent and the opaque states, respectively, below and above the transition temperature.

An interesting behavior of SCMO is the modulation of the T_{CO} versus Sm content. Indeed, the Mn^{3+} enrichment in the $CaMnO_3$ parent compound depends on the Sm addition, which gradually incorporates mobile electrons in the e_g band and decreases the electrical resistivity. The interaction of these carriers through the t_{2g} electron spins induced a ferromagnetic (FM) coupling and a metallic behavior.[7] However, a tendency to a charge order and therefore an antiferromagnetic insulating (AFMI) state occurs with the Mn^{4+} increase. As a consequence, the competition of these two opposite effects promotes the electronic transport for low Mn^{4+} contents while the charge order becomes predominant for higher Mn^{4+} contents. In this way, the control of the Ca:Sm atomic ratio allows to adjust readily the electrical resistivity. Considering applications like IR furtivity, the T_{CO} has to take place close to the ambient temperature. Such temperatures are observed for intermediate contents with $0.5 \leq x \leq 0.6$. $Sm_{0.5}Ca_{0.5}MnO_3$ shows a semiconducting behavior around the room temperature and a semi-metallic behavior above the transition.[8] Although the thermochromic properties of SCMO materials have been studied in the bulk form, no information is related for SCMO thin films.[5] This work focused on the elaboration of $Sm_{0.5}Ca_{0.5}MnO_3$ coatings using reactive magnetron sputtering and on the ability of such manganite films to thermochromic applications in IR domain.

II. EXPERIMENT

Sm-Ca-Mn oxide films of 700 nm thickness have been deposited on double side polished intrinsic {100} silicon substrates. Thin films were obtained by magnetron co-sputtering process from a Mn target and a Sm-Ca composite metallic target (42%–58% in surface). The area of the mixed target and the sputtering conditions were first adjusted to reach an atomic ratio Sm:Ca of one. The substrates are successively cleaned in acetone and methanol activated by an ultrasonic bath and directly positioned on a rotating substrate holder positioned at 70 mm away from the targets. To reach a compound sputtering regime ensuring together the stability of the sputtering conditions in reactive plasma and the full oxidation of the sputtered atoms during the deposition step,[9] O_2 and Ar flow rates were fixed to 10 and 20 sccm, respectively. Within the pumping speed of the deposition chamber, the total pressure was fixed to 0.5 Pa. The (Ca+Sm)/Mn atomic ratio was adjusted according to the discharge current applied on the Mn target using a pulsed-dc Pinnacle+

a)Author to whom correspondence should be addressed. Electronic mail: Fabien.Capon@ijl.nancy-universite.fr.

Advanced Energy supply. The direct current applied on the Sm-Ca composite target was fixed at 0.48 A. The film stoichiometry was checked using energy dispersive spectroscopy (EDS) from a Phillips FEG-XL30S scanning electron microscope. Coating thickness was determined by the step method with a Talysurf profilometer allowing an accuracy of about 20–30 nm. X-ray investigations were performed on an Inel diffractometer ($\lambda = 0.154059$ nm, $CuK_{\alpha 1}$ radiation) in grazing angle of 4°. dc electrical measurements were realized in four probes configuration from liquid nitrogen temperature to 420 K. The infrared behavior versus temperature was studied using a Nicolet 6700 Fourier transform infrared (FTIR) spectrometer equipped with a deuterated triglycine sulfate (DTGS) detector in the 400–7000 cm^{-1} wavelength range (i.e., 1.24–25 μm). A Linkam THMS600 stage was appended in the sample compartment. The stage can achieve measurements from 77 K to 870 K with an accuracy of 0.5 K.

III. RESULTS AND DISCUSSIONS

A. Structural properties

As-deposited Sm-Ca-Mn-O thin films were amorphous and a post-annealing under ambient air during 15 h was necessary to induce the crystallization of the perovskite phase. The temperature of crystallization was optimized at 1070 K. This annealing temperature is much softer than that is usually necessary to crystallize bulk manganites.[4,10,11] A typical x-ray diffractogram of the annealed film is presented in Fig. 1.

The lattice constants were refined using the CELREF software and the following values were obtained as $a = 0.53702$ nm, $b = 0.75957$ nm, and $c = 0.53677$ nm. The orthorhombic *Pnma* space group is suggested.[12] Reducing this structure to a "pseudo-cubic structure" with average lattice parameters $a = \sqrt{2}.a_p$, $b = 2.a_p$, and $c = \sqrt{2}.a_p$, results to a pseudocubic parameter of 0.37960 nm, that is, in good agreement with Chen *et al.*[13] Polycrystalline randomly oriented films were obtained. Applying the Scherrer's formula, the average grain size is estimated close to 80 nm.

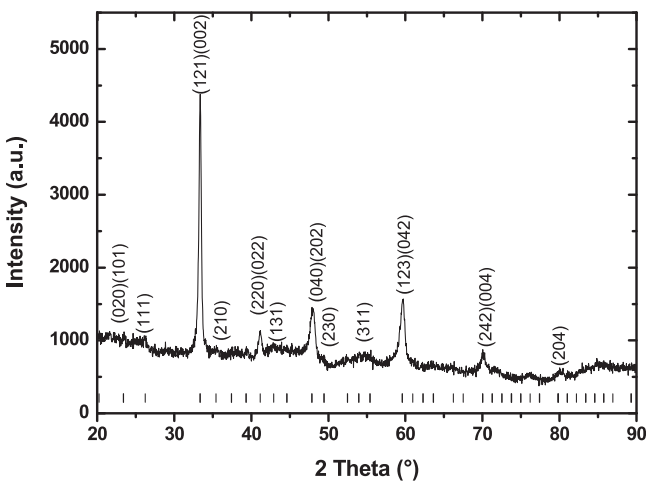

FIG. 1. X-ray diffraction pattern for a SCMO thin film deposited on Si(100) after annealing at 1070 K. Indexation refers to orthorhombic cell *Pnma* with average $a = \sqrt{2}.a_p$, $b = 2.a_p$, and $c = \sqrt{2}.a_p$ according to Qian *et al.*[12]

B. Electrical properties

Fig. 2 shows the electrical resistance of the SCMO annealed thin film according to the temperature. Increasing the temperature leads to a drop of the resistance. A transition of about two orders of magnitude is evidenced and a metallic state is clearly brought out for higher temperatures. Switching electrical characteristics are extracted from the derivative temperature curve presented in inset of Fig. 2. T_{CO} was determined for $d(\ln R)/dT = 0$ and corresponds to 325 K. This result is in good agreement with the magnetic phase diagram of SCMO established by Martin *et al.*[14] Indeed, increasing the temperature for intermediate compositions $0.35 \leq x \leq 0.85$, a transition occurs from the AFMI state to a paramagnetic semi-metallic (PMM) state. This CO transition is associated to a metal-insulator (MI) transition.[15]

C. Optical properties

To highlight a potential thermochromic effect in our films, dc electrical measurements are complemented by infrared transmission measurements.

At low temperature and below T_{MI}, the spectra in Fig. 3 show a typical semi-conductive behavior and reveal some absorptions bands. The band located at 16.6 μm (†) is related to the antisymmetric stretching $\nu_{Mn\text{-}O}$, whereas the band at 18.8 μm (‡) is driven by the deformation modes $\delta_{Mn\text{-}O}$ of the MnO_6 octahedra.[4] The renewed native oxide layers owing to the annealing treatment give rise to four absorption bands at 9.2 μm, 11.3 μm, 13.6 μm, and 16.3 μm, while the CO_2 and H_2O absorption activities are discernible. At the lower limit of the wavelength measurement range, the transmittance reaches 30% in the semiconductor state. In order to calculate the optical gap, the transmittance was investigated using a Cary UV-visible-NIR spectrometer in the 1–3 μm range and spectra are presented in inset of Fig. 4(a) for temperature ranging from 120 K to 470 K.

According to the inter-band absorption theory, the optical band gap of a film can be estimated from the extrapolation of the rising part of the Tauc's curve $(\alpha.h\nu)^{1/n} = f(h\nu)$.

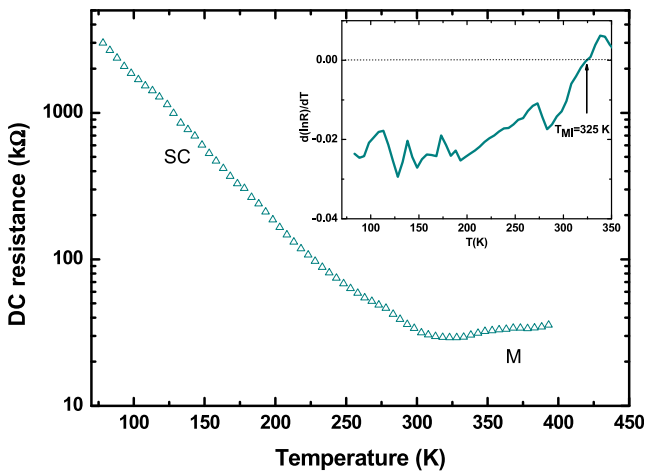

FIG. 2. Temperature dependence of the resistance of the SCMO annealed at 1070 K. The T_{CO} is defined when the derivative temperature curve changes its sign (inset). The dc electrical transition is clearly brought out for the highest annealing temperature.

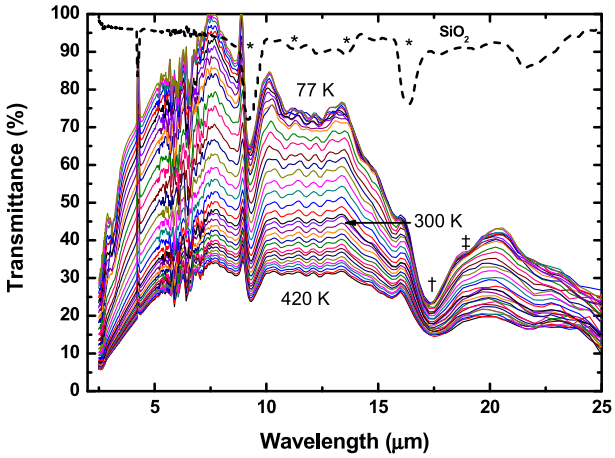

FIG. 3. Evolution of the infrared transmittance at different temperatures 77 K to 420 K for the SCMO coating annealed at 1070 K. The SiO_2 spectrum is represented in dashed line, stars (*) represent the absorption bands of the native silicon oxide layer related to the substrate, and † and ‡ show the absorption bands of the perovskite.

The value $\alpha = (1/t).\ln(1/T)$ corresponds to the absorption coefficient where t is the film thickness and T the transmittance. Different situations were investigated using n values of 2, 3, 1/2, and 3/2 for electronic transitions as indirect-allowed, indirect-forbidden, direct-allowed, and direct-forbidden transitions, respectively. The best fit was obtained for $n = 1/2$ whatever the temperature of the semiconducting phase. A typical Tauc's curve is presented for the IR transmittance spectrum measured at 120 K in Fig. 4(a) allowing the determination of the optical gap at Eg = 0.78 eV. All optical gap values versus temperature presented in Fig. 4(b) are comprised in the range 0.70–0.78 eV corresponding to the cut-off wavelengths 1.55–1.80 μm. Several models reported by authors[16,17] describe the energy gap as a function of temperature for a semiconductor. Among these, the Varshini model is often used for various III–V and II–VI semiconductors. Nevertheless, this model leads to an approximating fit at low temperature in most of cases. Another hand, its Debye temperature dependence is not well established. As an alternative, the Bose-Einstein model[17] is used

$$E_{og}(T) = E_{og}(0) - \frac{2\alpha_B}{\exp\left(\frac{\theta_E}{T}\right) - 1}, \qquad (1)$$

$Eg(0)$ is the band gap at the zero temperature and α_B is a parameter associated with the strength of the exciton-phonon interaction within the crystal. θ_E is average temperature of phonons coupled with the electronic subsystem. The Debye temperature (θ_D) for an Einstein oscillator can be estimated from the relationship $\theta_D = 4/3\ \theta_E$. The next two steps are to fit the data to the model we selected. First, the Debye temperature and the optical band gap at 0 K were arbitrary fixed at 500 K and 0.80 eV in order to refine α_B. The Debye temperature is intermediate between θ_D reported in Refs. 18 and 19 for $SmMnO_3$ and $CaMnO_3$ which correspond to 397 K and 774 K, respectively. Second, each parameter is varied in turn and refined using the least squares method. Although the explored temperature range does not entirely account for the asymptotic behaviour of the optical band gap at low

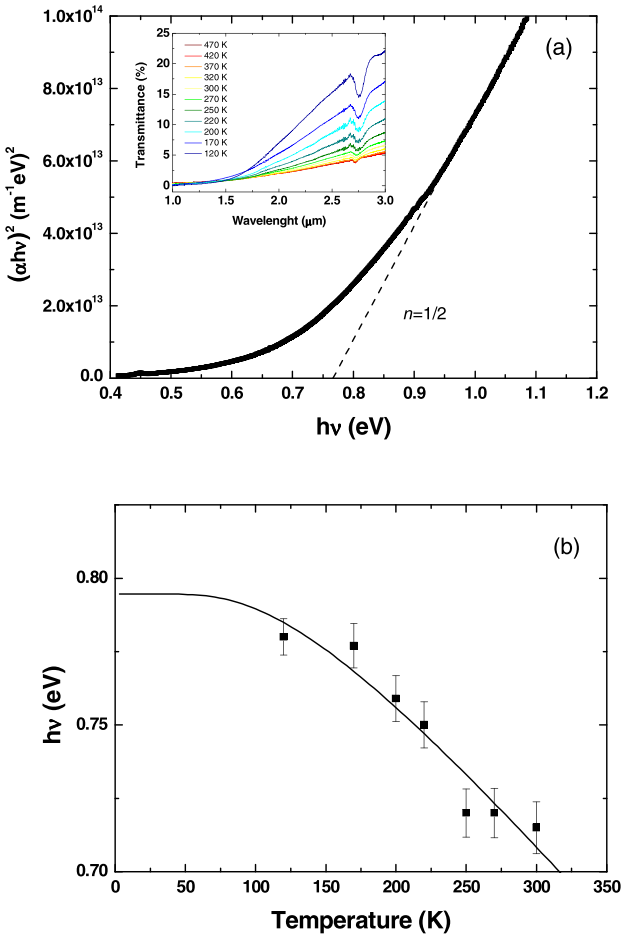

FIG. 4. Extrapolation of the rising part of the curve $(\alpha.h\nu)^{1/n} = f(h\nu)$ for a direct-allowed electronic transition ($n = 1/2$) from the NIR transmittance spectrum at 120 K is presented in (a). The NIR-visible range transmittance characterisation is clarified in inset. (b) The optical band gap versus temperature is reported in the semiconductor region. The optical band gap is found to be 0.7 eV near the transition temperature.

temperature, the optical band gap is refined to 0.79 ± 0.01 eV at 0 K ($\theta_D = 590$ K and $\alpha_B = 140$ meV).

Overall, regardless of temperature, the optical band gap appears to be intermediate between those usually calculated in thermochromic $NdNiO_3$ system (0.1 eV) and VO_2 (1.81 eV).[20,21] As a result, $Sm_{0.5}Ca_{0.5}MnO_3$ is optically active in the near infrared domain in band I and band II.

Considering the thermochromic efficiency versus temperature, above the transition temperature, the delocalization of electrons is promoted. This electronic behavior involves a screening effect for incident photons. In order to quantify this property, the average intensity of the bands $(1/\Delta\lambda)\int_{\lambda_2}^{\lambda_1} I(\lambda)/I_0.d\lambda$ was computed for each temperature (Fig. 5).

A progressive thermochromic effect is observed in the three bands. It is usual to define the optical contrast factor as $\tau(\lambda) = (\tau_{LT} - \tau_{HT})$, where τ_{LT} and τ_{HT} are transmittance at low and high temperatures, respectively, and λ is the IR wavelength. A band contrast factor $\tau(\Delta\lambda)$ for a given spectral band $\Delta(\lambda)$ characterizing the optical transmission switching efficiency can also be defined. The calculated band factor contrast is equal to 12%, 44%, and 55%, in BI, BII, and BIII,

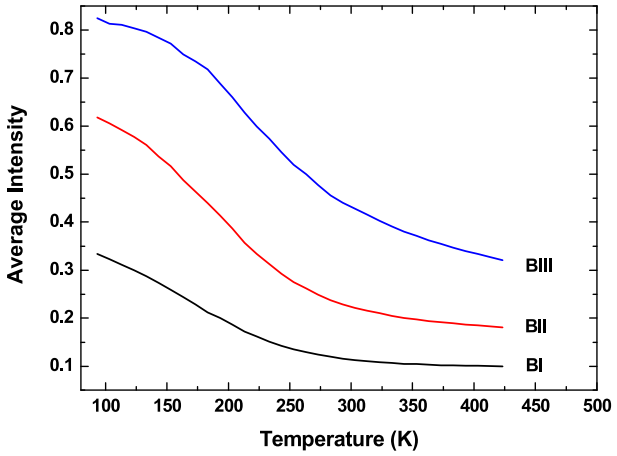

FIG. 5. This figure represents the average intensity versus temperature of the SCMO annealed at 1070 K for each transparency band of the atmosphere: band I (BI: 1–2.8 μm), band II (BII: 3–5 μm), and band III (BIII: 8–14 μm).

respectively. These results reveal a significant thermochromic contrast and confirm that the material is optically active in the near infrared range showing an original infrared switching in BI and BII.

IV. CONCLUSION

We have synthesized for the first time $Sm_{0.5}Ca_{0.5}MnO_3$ thin films by reactively co-sputtering of a composite Sm-Ca target and a pure Mn target. A post-annealing under ambient air at 1070 K is sufficient to induce the crystallization of the perovskite. dc electrical measurements exhibit a T_{MI} of 325 K associated with a thermochromic contrast. The optical band gap estimated at 0.7 eV brings the thermochromic effect into the range of the atmosphere transparency band I, band II, and band III with a contrast of 12%, 44%, and 55%, respectively.

These results may allow to devices the ability to operate in the far infrared region and are very promising for potential applications such as detection or temperature regulation systems operating in this spectral range.

[1]D. A. Filippov, R. Z. Levitin, A. N. Vasil'ev, T. N. Voloshok, H. Kageyama, and R. Suryanarayanan, Phys. Rev. B **65**, 100404 (2002).
[2]A. N. Vasil'ev, T. N. Voloshok, and R. Suryanarayanann, JETP Lett. **73**(7), 349 (2001).
[3]B. M. Ferreira, M. E. Melo Jorge, M. E. Lopes, M. R. Nunes, and M. I. da Silva Pereira, Electrochim. Acta **54**, 5902 (2009).
[4]P. Laffez, M. Zaghrioui, L. Reversat, and P. Ruello, Appl. Phys. Lett. **89**, 081909 (2006).
[5]P. Laffez, C. Napierala, M. Zaghrioui, V. Ta Phuoc, A. Hassini, and M. R. Ammar, Appl. Phys. Lett. **93**, 1 (2008).
[6]M. R. Ammar, C. Napierala, and P. Laffez, Smart Mater. Struct. **18**, 055002 (2009).
[7]C. Martin, A. Maignan, F. Damay, M. Hervieu, and B. Raveau, J. Solid State Chem. **134**, 198 (1997).
[8]V. Sivasubramanian, M. V. Rama Rao, T. Shripathi, V. Subramanian, and V. R. K. Murthy, Mater. Sci. Eng., B **77**, 128 (2000).
[9]F. Capon, D. Horwat, J. F. Pierson, M. Zaghrioui, and P. Laffez, J. Phys. D: Appl. Phys. **42**, 182006 (2009).
[10]G. M. Zhao, K. Conder, H. Keller, and K. A. Müller, Phys. Rev. B **62**(9), 5334 (2000).
[11]J. López and O. F. de Lima, Phys. Rev. B **66**(21), 214402 (2002).
[12]T. Qian, G. Li, Q. Han, X. Y. Guo, Y. Liu, J. F. Qu, and X. G. Li, J. Appl. Phys. **95**(3), 977 (2004).
[13]Y. Z. Chen, J. R. Sun, J. L. Zhao, J. Wang, B. G. Shen, and N. Pryds, J. Phys.: Condens. Matter **21**, 442001 (2009).
[14]C. Martin, A. Maignan, M. Hervieu, and B. Raveau, Phys. Rev. B **60**(17), 12191 (1999).
[15]J. Hejtmánek, Z. Jirák, M. Maryško, C. Martin, A. Maignan, M. Hervieu, and B. Raveau, Phys. Rev. B **60**(20), 14057 (1999).
[16]K. P. O'Donnell and X. Chen, Appl. Phys. Lett. **58**, 25 (1991).
[17]P. K. Sarswat and M. L. Free, Physica B **407**, 108 (2012).
[18]G. Lalitha and P. Venugopal Reddy, J. Magn. Magn. Mater. **320**, 754 (2008).
[19]A. Srivastava and N. K. Gaur, J. Phys.: Condens. Matter **21**, 096001 (2009).
[20]F. Capon, P. Ruello, J. F. Bardeau, P. Simon, P. Laffez, B. Dkhil, L. Reversat, K. Galicka, and A. Ratuszna, J. Phys.: Condens. Matter **17**, 1 (2005).
[21]Z. F. Luo, Z. M. Wu, X. D. Xu, T. Wang, and Y. D. Jiang, Chin. Phys. B **19**(10), 106103 (2010).